6 kW Single Stage Narrow Linewidth Fiber Amplifier Based on the Balance Between Mode Instability and Nonlinear Effects

Xin Tian, Binyu Rao, Meng Wang, Xiaoming Xi, Baolai Yang, Zilun Chen, Hu Xiao, Xiaolin Wang, Pengfei Ma, Zefeng Wang, and Jinbao Chen

***Abstract*—Single-stage high-power narrow-linewidth fiber laser has been investigated intensively recently because of its simple and robust configuration and great potential in spectral/coherent beam combination. In this work, a 6 kW narrow-linewidth fiber amplifier was experimentally achieved based on a fiber oscillator seed. By employing a few-mode ytterbium-doped fiber, the spectral broadening and SRS effects are both significantly mitigated. Combined with a wavelength-stabilized 981 nm pump source, the threshold of transverse mode instability is improved, then, a maximum output power of 6020 W at the central wavelength 1080 nm was achieved with 3-dB bandwidth of ∼0.37 nm and optical-to-optical efficiency of ∼85.6%. The mode instability and nonlinear effects were balanced well. The measured beam quality and the signal to Raman ratio were M^2∼2.7 and ∼27 dB, respectively. This work shows the great potential of such amplification structure for the power scaling of high-power narrow-linewidth fiber lasers.**

***Index Terms*—Fiber lasers, laser amplifiers, nonlinear effects.**

I. Introduction

HIGH power narrow-linewidth fiber lasers (NLFLs) play an important role in spectral/coherent beam combinations, which are helpful for expanding single fiber output power [1], [2]. Recently, the power scaling of high-power NLFLs has been investigated intensively. It is challenging for power scaling in a NLFL since transverse mode instability (TMI) effect and various nonlinear effects, such as four wave mixing (FWM), self-phase modulation (SPM), stimulated Brillouin scattering (SBS), and stimulated Raman scattering (SRS). Furthermore, due to the high spectral density the thresholds of nonlinear effects are much lower than those in traditional high-power fiber lasers, whose linewidth are usually more than several nanometers.

Normally, high power NLFLs can be acquired by using a structure of master oscillator power amplification (MOPA), in which the seed is a narrow-linewidth laser. There are two promising kinds of seed sources, i.e., phase-modulated single-frequency lasers and fiber Bragg grating (FBG)-based oscillators. The front has shown a good time domain characteristic and so its spectral broadening and SRS effects are weak relatively during the power amplification [3], [4], [5]. Some breakthroughs have been made recently [6], [7], [8]. In 2021, Huang et al. achieved the output power of 5.07 kW narrow linewidth continuous wave fiber amplifier with near diffraction limit beam quality and 0.37 nm 3 dB linewidth [7]. In 2022, Wang et al. achieved a 6.12 kW record narrow-linewidth fiber laser with 0.86 nm bandwidth and near single mode beam quality [8]. However, the SBS threshold of the single frequency seed is very low and thus need a complicated and expensive multi-stages configuration to widen signal linewidth to increase the SBS threshold [9]. MOPA based on oscillator seed consists of single stage amplification structure. It is an alternate solution to obtain high power NLFLs with lower cost and better robustness. The characteristic of less longitudinal modes in this type of seed makes it almost unnecessary to consider SBS effect. However, the resulting spectral broadening is more serious than single-frequency phase-modulated laser seed [10]. And SRS effect induced by instability in temporal domain is one of the biggest obstacles for power boosting in the single stage MOPA structure NLFLs [5]. However, its obvious advantage of simple structure is worthy studying and has attracted intensive attention

Up to now, the average output power of this type of NLFL has reached to 3∼4 kW level [10], [11], [12], [13], [14], [15]. In 2022, Du et al. reported a 0.4 nm, 3.3 kW output power from a backward pumped fiber amplifier and the beam quality was M^2 ∼1.32 [13]. Then, our previous work achieved an output power of 4.2 kW single mode narrow linewidth fiber amplifier with 3 dB linewidth of 0.62 nm [15]. In these studies, the power scaling is always accompanied by a process of balancing nonlinear effects and TMI. Because there are certain contradictions when using traditional design strategies to suppress TMI and nonlinear effects. For instance, weakening heat load along the active fiber could enhance the TMI threshold, whereas the longer YDF

Manuscript received 25 May 2023; revised 19 July 2023; accepted 18 August 2023. Date of publication 22 August 2023; date of current version 11 September 2023. This work was supported in part by the National Natural Science Foundation of China under Grants 11974427 and 12004431, in part by the State Key Laboratory of Pulsed Power Laser under Grants SKL2020ZR05 and SKL2021ZR01, and in part by the Postgraduate Scientific Research Innovation Project of Hunan Province under Grant CX20210021. *(Corresponding authors: Xiaoming Xi; Zefeng Wang.)*

The authors are with the College of Advanced Interdisciplinary Studies, National University of Defense Technology, Changsha 410073, China, and with the Nanhu Laser Laboratory, National University of Defense Technology, Changsha 410073, China, and also with the State Key Laboratory of Pulsed Power Laser Technology, Changsha 410073, China (e-mail: exixiaoming@163.com; zefengwang_nudt@163.com).

Digital Object Identifier 10.1109/JPHOT.2023.3307580

required in this case would strengthen the SBS and SRS effects and broaden the output spectrum. Besides, a large core diameter of the fiber could mitigate the SRS and spectral broadening effects, but at the same time higher-order modes (HOMs) would be introduced so that increasing the danger of the TMI and FWM effects. Moreover, TMI and nonlinear effects are usually interrelated in high-power continuous wave fiber lasers [17], [18], [19]. Therefore, comprehensive method balancing TMI and nonlinear effects for further power scaling of high-power fiber lasers and amplifiers becomes an imminent necessity.

In this work, we have experimentally demonstrated a 6-kW narrow-linewidth one-stage MOPA fiber laser based on a fiber oscillator seed. The fiber amplifier adopts a custom-made wavelength-stabilized 981 nm pump source to enhance the TMI threshold. Besides, the active fiber of amplifier stage with a large mode area of 30 μm is employed to mitigate SRS and spectral broadening effects. By this way, the TMI and SRS effects are effective balanced. At the maximum laser power of 6020 W, the optical-to-optical (O-O) efficiency is 85.6%, and the measured 3-dB and 10-dB linewidths are 0.37 nm and 1.47 nm, respectively. The Raman suppression ratio is ∼27 dB. Because of the large core size of the fiber, the output laser operates in a multimode regime and the measured M^2 is ∼2.7 at the maximum power.

II. Experimental Design and Setup

For the design of the oscillator seed, the reduced longitudinal mode number of the seed is the key to narrower linewidth of the amplifier [10]. In a laser cavity, the longitudinal mode interval can be derived as $\Delta\upsilon = c_0/2nL$, where $\Delta\upsilon$ denotes the longitudinal mode interval, c0 is the light speed in vacuum, n is the refractive index of silica fiber, and L is the length of cavity. It indicates that a shorter cavity implies a larger $\Delta\upsilon$ and small number of longitudinal modes. Therefore, here the seed oscillator was adopted with a short resonant cavity with an active fiber length of 3 m. And a narrow-linewidth FBG with a full-width-at-half-maximum (FWHM) of 0.04 nm was adopted. Besides, a seed laser with good temporal characteristics is helpful to suppress SRS effect in the fiber amplifier because fewer pulses with high peak of laser is amplified. During experimental exploration, it was found that a broader bandwidth of high reflector (HR) FBG could mitigating the SRS effect induced by polarization dependence. The mechanism can be explained that the polarization-mode-interacted FWM (PFWM) would be easier to be excited in oscillator containing HR-FBG with wide bandwidth or fiber with a larger core ellipticity [20]. Besides, the PFWM-induced polarization dispersion would cut the Raman gain down due to the polarization variation of both signal and Raman laser so that elevate SRS threshold [21]. Thus, a HR-FBG with a relatively broad FWHM of 2.6 nm was utilized in the seed. In addition, the reasonable seed power is also the key for suppressing SRS, it neither be too low, otherwise a sustained self-pulsing of seed laser could be strong in the time domain; nor be too high, as the SRS noise of seed laser would be amplified [15].

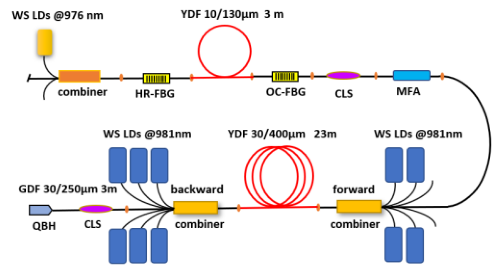

Fig. 1. Schematic of the narrow-linewidth single-stage MOPA fiber laser.

For the design of the amplification stage, it needs to comprehensively weigh the influence of the nonlinear effects and the TMI. In this NLFL, the SBS is no need to pay more attention because the signal linewidth is widened enough during the seed laser transmitting long fiber of amplifier. However, other nonlinear effects such as SRS, FWM, combined with TMI effect would restrict the spectral purity and improvement of output power. Besides, the spectral broadening effect of signal light need to be controlled. Here, we balance SRS, spectral broadening and TMI effects by increasing the core size of fiber in the amplification stage, combined with optimizing the pump wavelength, that is 981 nm. Large core size fiber could mitigate SRS effect and spectrum broadening but decrease the TMI threshold with conventional pump wavelength of 976 nm. The pump wavelength of 981 nm could reduce heat load along active fiber for relatively low pump absorption, thus increasing the threshold of TMI compared to the case that using pump wavelength of 976 nm, while the needed active fiber is longer than pump wavelength of 976 nm but shorter than that pump wavelength of 915 nm [22]. Furthermore, the pump direction and pump power distribution also have an impact on SRS and TMI thresholds. Adopting counter-pumped configuration is helpful to mitigate SRS effect, because signal laser with high power only transmits by relatively short length of the fiber, which reduces the effective fiber length of high-power fiber lasers. But TMI effect would block the improvement of output power if only with the sole counter-pumped. Instead, the bidirectional configuration offers an advantage on redistributing heat load in active fiber and thus improving the final output power.

Based on the above design strategies, the single-stage MOPA configuration fiber laser based on FBG-seeded is illustrated in Fig. 1. A wavelength stabilized 976 nm laser diode (LD) was used as the pump source of seed. A pair of FBGs with center wavelength of 1080 nm and 3 m long ytterbium-doped fiber (YDF) form the resonant cavity of oscillator. The HR-FBG has a reflectivity of 99.5% and a FWHM of 2.6 nm. The OC-FBG provides a reflectivity of 10% and a FWHM of 0.04 nm. The used active fiber has a size of 10/130 μm with the absorption coefficient of 1.4 dB/m at 915 nm. After the fiber oscillator seed, there is a mode-field adaptor (MFA) connecting amplifier stage. The input and output signal fiber of MFA have core and inner cladding of 10/130 μm and 30/250 μm respectively.

The main amplifier is based on a bidirectional-pump configuration by adopting two (6+1) ×1 pump/signal combiners (PSC). The pump source of amplifier adopted multiple groups

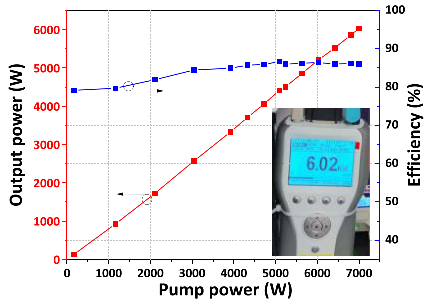

Fig. 2. Optical-to-optical efficiency of fiber laser and the variation of output power with the increase of pump power.

of wavelength-stabilized 981 nm LDs. Each group LDs can provide a maximum power of ∼900 W. The pump fibers of the PSC are multimode fibers with size of 200/220 μm and core NA of 0.22. The input and output signal fibers size of the PSC are 30/400 μm and 30/250 μm. The active is large mode area YDF with core/ inner cladding of 30/400 μm and a core NA of 0.06. The pump absorption coefficient of the YDF is about 0.8 dB/m at the wavelength of 981 nm. The length of the YDF of amplifier stage is about 23 m. The YDF was coiled with a minimum radius of 12 cm and a maximum radius of 16 cm in the grooves on a water-cooled heat sink. The selection of coiling radius is to balance TMI threshold and beam quality [23]. When bending diameter is larger than 12 cm, the MI threshold would be improved with deterioration of beam quality; with smaller coiling radius, the beam quality could maintain well but the MI threshold would decrease. The residual pump light was removed by a cladding light stripper (CLS). The laser was ultimately transmitted in a fiber with a core/cladding diameter of 30/250 μm and output by a quartz block head (QBH) in the end. In the all-fiberized laser system, effective heat management was realized by cooling all fiber devices and perfect fusions, making sure the stability of fiber laser system in high power operation. The performance of the NLFL including output power, signal linewidth, optical spectrum and beam quality were measured and recorded in the experiment

III. Experimental Results and Discussion

According to the selection principle of seed power mentioned above, here the seed power was set about 30 W considering the timing domain and SRS noises of fiber oscillator seed. The spectrum was measured by an optical spectrum analyzer with a spectral resolution of 0.02 nm and the FWHM of the seed transmitting through the amplification stage was 0.28 nm. In the experiment, we firstly injected the backward pump and then forward pump to the main amplifier. Under a total pump power of 7000 W, we achieved the maximum laser output power of 6020 W. As shown in Fig. 2, the output power and optical-optical efficiency versus pump power are depicted respectively. The O-O conversion efficiency of this NLFL did not decrease during the increase of output power, and this value was 85.6% at the maximum power.

The measured spectra at different output powers are depicted in Fig. 3(a). The central wavelength of the signal laser remains

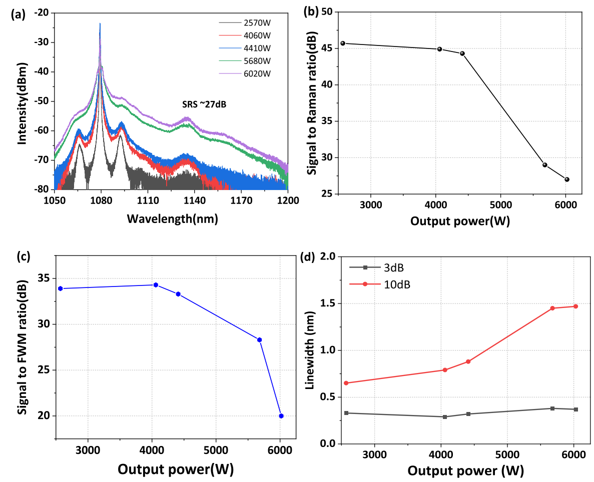

Fig. 3. (a) The laser spectrum at different output powers (b) The evolution of SRR versus output power (c) The evolution of signal to FWM ratio versus output power (d) The evolution of 3 dB and 10 dB linewidths of signal laser.

almost stable in the experiment. It can be observed the obvious FWM in the output spectrum. With only backward pump of 5235 W injecting, the output power reached 4400 W with the signal to Raman ratio (SRR) of 44 dB. The signal to FWM ratio (SFR) was about 33 dB. Then when the output power exceeded 4400 W, there was a serious spectral broadening at the bottom of the signal spectrum arising from self- and cross-phase modulation effects. In addition, the Stokes light and anti-Stokes light were also amplified with the enhancement of the nonlinear interaction. But the Stokes line and anti-Stokes line were unequally which can be attributed to the SRS effect [24]. With the forward pump light of 1765 W added, that is a total pump power of 7000 W, the output power reached the maximum value of 6020 W with SRR of 27 dB. The FWM ratio at 1092 nm is about 20 dB at the highest output power of 6020 W. The evolution of SRR and SFR versus output power are displayed in Fig. 3(b) and (c), respectively. Whether the SRR or SFR, the signal component decreased quickly with the additional forward pump injecting. The SRR decreased from 44 dB at 4400W to 27 dB at 6020 W and SFR decreased from 30 dB to 20 dB under the same circumstances. Fig. 3(d) shows the evolution of 3-dB and 10-dB bandwidth with output power increasing. The bandwidth increases almost linearly with only the backward pumped then this trend became steep with increasing forward pump. At the highest power of 6020 W, the 3-dB and 10-dB bandwidth reached up to 0.37 nm and 1.47 nm.

From the output spectrum of 2570 W, we can infer the threshold of FWM is lower than SRS effect. This because the optical parametric gain of FWM is higher than the peak of Raman gain in this large mode area fiber that satisfied phase matching. In fiber lasers, the strong intermodal FWM effect arises from the phase matching between the fundamental mode and HOMs [25], [26]. Due to the momentum conservation, the wave numbers of two generated photons must be of opposite signs. The real propagation constant of LP_{mn} mode can be derived as

$$\beta_{\mathrm{mn}}|_f = n_{mn}(f)2\pi f/c = [n_{core}(f) + \Delta n_{mn}(f)] \times 2\pi f/c$$

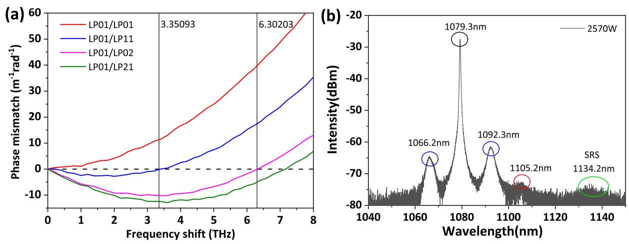

Fig. 4. (a) The phase matching conditions between different modes. (b) The experimental output spectrum at 2570 W.

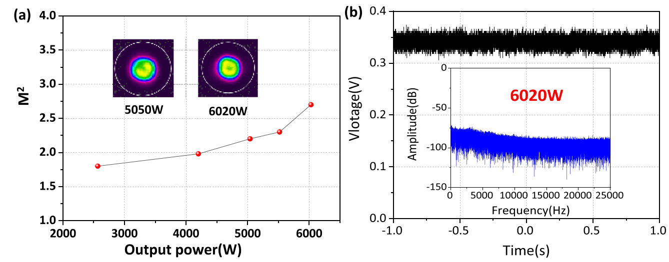

Fig. 5. (a) The evolution of beam quality versus laser output power. (b) The temporal signal and corresponding fourier spectrum at 6020 W.

where n_{mn} is the mode effective index. The first term contains the material dispersion, the later one contains waveguide dispersion and mode dispersion. Assuming the anti-Stokes light is the fundamental mode with a frequency shift of $+\Delta f$, and the Stokes light is the same higher-order mode with the frequency shift of $-\Delta f$. The frequency of the signal light is $f_{0.}$ The phase matching $\Delta\beta$ can be derived as

$$\Delta\beta = \beta_{mn}|_{f=f_0-\Delta f} + \beta_{01}|_{f=f_0+\Delta f} - \beta_{mn}|_{f=f_0} - \beta_{01}|_{f=f_0}$$

For the adopted fiber with core diameter of 30 μm and NA of 0.06, the normalized frequency parameter, i.e., V parameter, is calculated about 5.23 at the wavelength of 1080 nm, which indicates that five modes can be supported for simultaneous transmission including LP_{01}, LP_{02}, LP_{11}, LP_{12}, and LP_{31}. Fig. 4(a) depicts the calculated phase mismatch for a few mode fiber with propagation constant of V = 5.23. One pump light is the fundamental mode with wavelength of 1080 nm, and the other pump light is one of the HOMs. In this case, the phase matching condition is satisfied at $\Delta f = 3.35$ THz between LP_{01} and LP_{11} mode. When pumped at 1079.3 nm, the calculated anti-Stokes and Stokes wavelengths are 1066.4 nm and 1092.5nm. The discrepancy might result from choosing of the fiber parameter. This is in accordance with the experimental results, as shown by the blue mark in Fig. 4(b). Besides, there are also slightly envelope of about 1105.2 nm in the output spectra, as shown by the red mark, which corresponding to phase mismatch between LP_{01} and LP_{02} mode, and $\Delta f = 6.3$ THz. Whereas it is submerged in spectral broadening with increasing the output power, as shown in the spectrum in Fig. 3(a). Consequently, the intermodal FWM effect mainly occurs between the fundamental mode and the secondary mode in fiber lasers. The green mark in Fig. 4(b) shows the SRS effect, whose center wavelength is $\sim$ 1134.2 nm.

During the process of power amplification, we used a photodetector and an oscilloscope to record the temporal characteristics of laser. The beam quality was also measured simultaneously by a M^2 analyzer (Ophir Photonics, Beam Squared SP920). Fig. 5(a) shows the beam quality evolution. Because of large core size of the fiber adopted, the output laser operated in a multimode regime. Under the influence of TMI and FWM effects, the output laser spot jitters continuously, resulting in the gradual deterioration of the beam quality. And the M^2 factor is measured $\sim$2.7 at the maximum power of 6020 W. From the contour image of beam waist spot, one can see that the output laser mode is mainly composed of fundamental mode (LP_{01}) and higher-order mode (LP_{11}). The slight fluctuations of the temporal signal and corresponding Fourier spectrum of the dumped cladding is observed at the maximum power, as shown in Fig. 5(b), reasonably indicating TMI effect occurred [27]. Therefore, TMI is the direct obstacle for further power scaling of this NLFL.

Next, the experimental design strategies will focus on improving beam quality and mitigating the TMI and FWM effects for a higher output power. And suppressing inter mode FWM effect and optimizing beam quality are complementary. The essence of these problems is to decrease or control the number of modes in fiber. Some methods are proposed such as using the specially designed active fiber with low NA or vary core to achieve near single mode laser transmission [28]. In addition, mode control technology can also be used to suppress FWM effect in fiber laser, including gain fiber winding, gain fiber taper and mode conversion, and so on [29], [30]. Bending gain fiber is the simplest and easiest way to operate. In high-power fiber lasers and amplifiers, the bending loss of HOMs is greater than that of fundamental mode, appropriate winding radius could effectively reduce the proportion of high-order modes in fiber core for suppressing FWM and TMI effects.

In addition, the temporal characterizes of injected seed laser is the key to maintain narrow linewidth during the process of amplification. Although the linewidth of the laser decreases with reducing the longitudinal mode number of the seed source [10]. But the number of longitudinal modes is not the essential difference between phase modulated seed and multi-longitudinal modes oscillator seed. Two types of seeds possess different random phase distribution of the multiple waves or temporal features, thus, the multi-longitudinal mode seed experiences serious spectrum broadening induced by the self-phase modulation and FWM among various longitudinal modes. While the phase modulated seed can almost maintain the spectrum profile during the amplifying process even with some noise fluctuation [31]. Some methods to enhance temporal stability of oscillator have been proposed such as utilizing composite cavity structure oscillator [32]. These factors would be considered in the future work.

IV. Conclusion

In conclusion, we have experimentally demonstrated a high-power bidirectional pump narrow-linewidth single-stage MOPA system. The adopted large mode area active fiber with 981 nm pump wavelength help to obtain an output power of more than 6 kW. The O-O conversion efficiency is $\sim$85.6%, the FWHM bandwidth is ∼0.37 nm, and the SRR is ∼27 dB. The laser has operated at 6 kW for ∼3 mins and the calculated power instability was less than 1%. Because of the large core size of the fiber, the output laser operates in a multimode regime and the signal laser generates sideband energy. In the future work, the optimization of the seed's time domain characteristics and the improvement of beam quality are the key points. In short, this work shows a good potential of such simple amplification structure for power amplification of high-power NLFLs.

REFERENCES

[1] T. H. Loftus et al., "Spectrally beam-combined fiber lasers for high-average-power applications," *IEEE J. Sel. Topics Quantum Electron.*, vol. 13, no. 3, pp. 487–497, May–Jun. 2007.

[2] Z. Liu et al., "High-power coherent beam polarization combination of fiber lasers: Progress and prospect [Invited]," *J. Opt. Soc. Amer. B*, vol. 34, 2017, Art. no. A7.

[3] R. Su et al., "2.43 kW narrow linewidth linearly polarized all-fiber amplifier based on mode instability suppression," *Laser Phys. Lett.*, vol. 14, 2017, Art. no. 085102.

[4] T. Li, C. Zha, Y. Sun, Y. Ma, W. Ke, and W. Peng, "3.5, kW bidirectionally pumped narrow-linewidth fiber amplifier seeded by white-noise-source phase-modulated laser," *Laser Phys.*, vol. 28, no. 10, 2018, Art. no. 105101.

[5] H. Lin et al., "3.7 kW monolithic narrow linewidth single mode fiber laser through simultaneously suppressing nonlinear effects and mode instability," *Opt. Exp.*, vol. 27, no. 7, pp. 9716–9724, 2019.

[6] P. Ma et al., "All-fiberized and narrow-linewidth 5 kW power-level fiber amplifier based on a bidirectional pump configuration," *High Power Laser Sci. Eng.*, vol. 9, 2021, Art. no. e45.

[7] Z. M. Huang et al., ">5kW record high power narrow linewidth laser from traditional step-index monolithic fiber amplifier," *IEEE Photon. Technol. Lett.*, vol. 33, no. 21, pp. 1181–1184, Nov. 2021.

[8] G. Wang et al., "Six kilowatt record all-fiberized and narrow-linewidth fiber amplifier with near-diffraction-limited beam quality," *High Power Laser Sci. Eng.*, vol. 10, 2022, Art. no. e22.

[9] M. Hekmat, M. Mozdoor Dashtabi, S. Manavi, E. Hassanpour Yesaghi, and R. Massudi, "Study of the stimulated Brillouin scattering power threshold in high power double-clad fiber lasers," *Laser Phys.*, vol. 23, 2013, Art. no. 012025.

[10] Y. Wang et al., "Effect of the number of longitudinal modes on spectral broadening in a high power fiber amplifier," *IEEE Photon. Technol. Lett.*, vol. 30, no. 12, pp. 1107–1110, Jun. 2018.

[11] Z. Huang, X. Liang, Chengyu, L. L., Q. Li, J. Wang, and F. Jing, "Spectral broadening in high-power Yb-doped fiber lasers employing narrow-linewidth multi longitudinal-mode oscillators," *Appl. Opt.*, vol. 55, no. 2, pp. 297–302, 2016.

[12] Y. Wang et al., "3 kw, 0.2 nm narrow linewidth linearly polarized all-fiber laser based on a compact MOPA structure," *Laser Phys. Lett.*, vol. 17, no. 7, 2020, Art. no. 075101.

[13] Y. Huang et al., "3 kw narrow linewidth high spectral density continuous wave fiber laser based on fiber Bragg grating," *Opt. Laser Technol.*, vol. 133, 2021, Art. no. 106538.

[14] S. Du et al., "3.3kW narrow linewidth FBG-based MOPA configuration fiber laser with near-diffraction-limited beam quality," *Opt. Fiber Technol.*, vol. 73, 2022, Art. no. 103011.

[15] X. Tian, B. Rao, M. Wang, X. Xi, C. Wang, and Z. Wang, "4 kW narrow-linewidth fiber laser based on a simple one-stage MOPA structure," *Laser Phys. Lett.*, vol. 19, no. 11, 2022, Art. no. 115101.

[16] X. Tian, B. Rao, X. Xi, M. Wang, C. Wang, and Z. Wang, "Selection principle of seed power in high-power narrow linewidth fiber amplifier seeded by a FBGs-based fiber oscillator," *Opt. Exp.*, vol. 31, no. 8, pp. 12016–12025, 2023.

[17] K. Hejaz et al., "Modal instability induced by stimulated Raman scattering in high-power Yb-doped fiber amplifiers," *Opt. Lett.*, vol. 42, no. 24, pp. 5274–5277, 2017.

[18] Q. Chu et al., "Experimental study of mode distortion induced by stimulated Raman scattering in high-power fiber amplifiers," *Photon. Res.*, vol. 8, no. 4, pp. 595–600, 2020.

[19] W. Gao et al., "Effective suppression of mode distortion induced by stimulated Raman scattering in high-power fiber amplifiers," *High Power Laser Sci. Eng.*, vol. 9, 2021, Art. no. e20.

[20] B. Rao et al., "Stimulated Raman scattering suppression by intensified four-wave mixing process in narrow-linewidth fiber oscillator," *Opt. Laser Technol.*, vol. 164, 2023, Art. no. 109475.

[21] R. H. Stolen, "Polarization effects in fiber Raman and Brillouin lasers," *IEEE J. Quantum Electron.*, vol. 15, no. 10, pp. 1157–1160, Oct. 1979.

[22] B. Yang et al., "6 kW single mode monolithic fiber laser enabled by effective mitigation of the transverse mode instability," *Opt. Exp.*, vol. 29, no. 17, pp. 26366–26374, 2021.

[23] Y. Wen et al., "Experimental study on transverse mode instability characteristics of few-mode fiber laser amplifier under different bending conditions," *IEEE Photon. J.*, vol. 14, no. 4, Aug. 2022, Art. no. 1539106.

[24] J. Zheng et al., "Four-wave mixing effect on high-power continuous-wave all-fiber lasers," *Mod. Phys. Lett. B*, vol. 32, no. 23, 2018, Art. no. 1850275.

[25] L. Yin, Z. Han, H. Shen, and R. Zhu, "Suppression of inter-modal four-wave mixing in high-power fiber lasers," *Opt. Exp.*, vol. 26, no. 12, pp. 15804–15818, 2018.

[26] Q. Chu et al., "Experimental study of the influence of mode excitation on mode instability in high power fiber amplifier," *Sci. Rep.*, vol. 9, no. 1, 2019, Art. no. 9396.

[27] R. M. Tao et al., "Dynamic characteristics of stimulated Raman scattering in high power fiber amplifiers in the presence of mode instabilities," *Opt. Exp.*, vol. 26, no. 19, pp. 25098–15110, 2018.

[28] L. Zeng et al., "5 kW monolithic fiber amplifier employing home-made novel spindle-shaped ytterbium-doped fiber," *Opt. Lett.*, vol. 46, pp. 1393–1396, 2021.

[29] F. Zhang et al., "Bending diameter dependence of mode instabilities in multimode fiber amplifier," *Laser Phys. Lett.*, vol. 16, 2019, Art. no. 035104.

[30] R. Tao, R. Su, P. Ma, X. Wang, and P. Zhou, "Suppressing mode instabilities by optimizing the fiber coiling methods," *Laser Phys. Lett.*, vol. 14, 2016, Art. no. 025101.

[31] Y. Feng et al., "Spectral broadening in narrow linewidth, continuous-wave high power fiber amplifiers," *Opt. Commun.*, vol. 403, pp. 155–161, 2017.

[32] S. Zhang et al., "Suppressing stimulated raman scattering by adopting a composite cavity in a narrow linewidth fiber oscillator," *Appl. Opt.*, vol. 60, no. 20, pp. 5984–5989, 2021.